Available online at www.sciencedirect.com
SCIENCE DIRECT
Polymer 47 (2006) 4068–4074
polymer
www.elsevier.com/locate/polymer

Poly(ethylene oxide)/clay nanocomposite: Thermomechanical properties and morphology

D. Ratna [a,b], S. Divekar [a,b], A.B. Samui [a,b], B.C. Chakraborty [a,b], A.K. Banthia [b,*]

[a] Naval Materials Research Laboratory, Shil-Badlapur Road, Anand Nagar PO, District Thane 421 506, Maharashtra, India
[b] Materials Science Center, IIT, Kharagpur 721302, West Bengal, India

Available online 17 April 2006

Abstract

Poly(ethylene oxide) (PEO)/clay nanocomposites were prepared by a solution intercalation method using chloroform as a solvent. The nanocomposites were characterised by X-ray diffraction (XRD), differential scanning calorimetry (DSC), hot-stage polarized optical microscopy (POM), Fourier transform infrared spectroscopy (FT-IR), tensile analysis, dynamic mechanical analysis (DMA) characterisation techniques. Formation of nanocomposite was confirmed by X-ray diffraction (XRD) analysis. A decrease in PEO crystallinity in case of nanocomposite, was confirmed by a decrease in the heat of melting and spherulite size as indicated by DSC and POM studies, respectively. Improvement in tensile properties in all respect was observed for nanocomposites with optimum clay content (12.5 wt%). DMA studies indicate an increase in loss peak temperature and broadening of loss peak as a result of clay intercalation.

Keywords: Poly(ethylene oxide); Nanocomposite; Morphology

1. Introduction

Polymer/clay nanocomposites (PCN) are a new class of hybrid materials, discovered by researchers at Toyota, Japan using organically modified clay and nylon matrix [1]. The history of the discovery polymer/clay nanocomposites has recently been highlighted by Kawasumi [2]. The attraction of PCN is the low cost and historical availability of clay and the well developed intercalation chemistry which makes it possible to achieve nanostructure from micron size filler as starting materials [3,4]. In general two idealized polymer layered silicate structures are possible: intercalated and exfoliated. In an intercalated nanocomposite the insertion of polymer into the clay structure occurs in a crystallographically regular fashion and few molecular layers of polymer typically occupy the gallery region. In contrast, in an exfoliated nanocomposite, the individual 1 nm thick clay layers are dispersed in a continuous polymer matrix and segregated from one another by average distances that depend on clay loading. The schematic representation of the two types of nanocomposites are shown in Fig. 1.

Initial works on polymer/clay nanocomposites was focussed on mainly for reinforcement [5,6] and improvement of barrier properties [7] and flammability [8] of polymer systems. Subsequent studies on conductive polymers [9], liquid crystal polymers [10] and polyether oxide [11] based nanocomposites show considerable promise for economical applications of polymer/clay nanocomposites.

Since, the poly(ethylene oxide)/clay (PEO/clay) system has been viewed as a potential material for solid polymer electrolyte (SPE) application in electrochemical battery [11,12], many studies have been done on PEO/clay nanocomposites [13–17]. The preparation methods used for preparing PEO/clay nanocomposites are solution intercalation [18,19], steady state annealing [20,21] and melt extrusion [22]. Shen et al. [23] compared the solution and melt intercalation and reported better reinforcement in case of solution. Solution intercalation facilitates production of thin films with polymer and oriented-clay intercalated layers. The driving force for polymer intercalation into a layered silicate from solution is entropy gained by desorption of solvent molecules which compensates for the entropy decrease the confined intercalated chain [24]. The matching of polarity (enthalpy factor) between the PEO and gallery surface of the organo clay (modified with alkyl ammonium cation) also favours the intercalation process. Organic modification of clay introduces hydrophobic character into the clay gallery surface and encourages the intercalation.

Chen et al. [25] have recently reported comparative sorption

* Corresponding author. Address: Materials Science Center, IIT, Kharagpur 721302, West Bengal, India
E-mail address: ajitbanthia2000@yahoo.co.in (A.K. Banthia).

0032-3861/$ - see front matter © 2006 Elsevier Ltd. All rights reserved.
doi:10.1016/j.polymer.2006.02.040

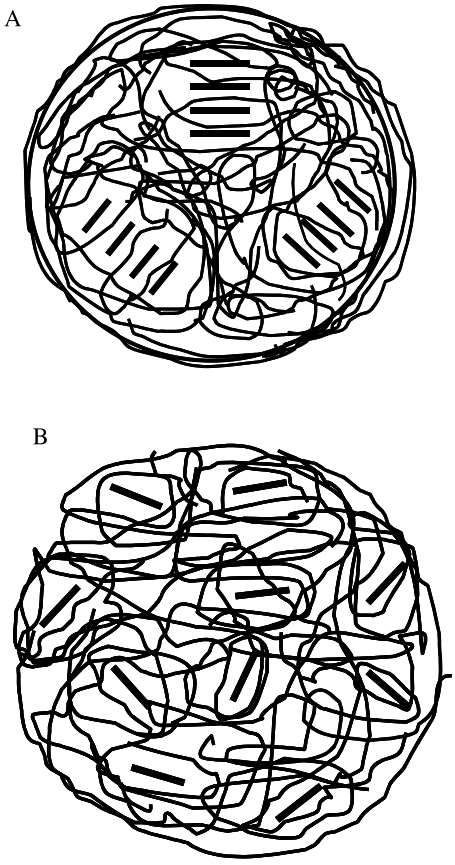

Fig. 1. Schematic representation of (A) intercalated and (B) exfoliated nanocomposite.

experiments for molar mass in polymer/clay nanocomposite and the results show that high molar mass fractions of polymer intercalate preferentially into smectite clay during solution intercalation method. High molecular mass is necessarily required for better thermal and mechanical properties. Many studies have focussed on the conformation on PEO chains in between the silicate clay layers. However, contradicting results have been presented, as several authors [23,26,27] reported on the existence of disturbed helical PEO crystal structure where as others consider PEO chain layers without any crystal structure formation [28].

PEO/clay nanocomposite compositions with excess clay (> 50 wt%) [29], as well as, with very low clay concentration (< 5 wt%) have been reported in the literature [22]. Optimum electrolyte properties are reported at about 8 wt% of clay [30]. Efforts have been mostly limited to the investigation of PEO/clay nanocomposites based on natural montmorillonite clay containing either Na^+ or ion-exchanged Li^+ in the intergallery spacing [26–28] or polar organo clay closite B-34 [22,23]. Unlike other polymer based nanocomposites the detailed thermomechanical properties and morphology using apolar clay has not been investigated.

The present work aims at the synthesis and characterization of PEO/clay nanocomposite using an apolar alkyl ammonium cations modified nanoclay. The detailed thermomechanical properties and morphology has been investigated to provide a good insight of the main parameters which can be manipulated in order to control the nanocomposite structure and thus properties of PEO/clay nanocomposite.

2. Experimental

2.1. Materials

The PEO with molecular weight of 600,000 g/mol was purchased from Aldrich. The organically modified clay used in this work was supplied by Nanocor Inc., IL, USA under the trade name of I 30E which was dried at 80 °C for 24 h under vacuum prior to use. The chloroform (AR grade) used was procured from SRL Chemicals Pvt. Ltd, India and used without further purification.

2.2. Preparation of nanocomposites

The organically modified clay was dispersed and swollen in chloroform for 24 h in a three necked flask at ambient temperature and was sonicated for 15 min. The PEO was then mixed in the flask and PEO/chloroform ratio 1:30 (g/ml) was maintained by adding an additional quantity of solvent. The flask, fitted with a condenser, a mechanical stirrer and a thermometer pocket was then placed in an oil bath heated to 75 °C. The mixture was kept under stirring condition for 10 h and was then sonicated for 30 min. Nanocomposites films were cast on a horizontal glass mould by pouring out the solution and dried in air overnight. The films were then dried at 55 °C under vacuum (<200 mbar) in a Heraeus Vacutherm oven for complete drying of the films for 24 h. A schematic overview of the nanocomposites synthesis is shown in Fig. 2. In order to study the effect of sonication samples were made with and without sonication.

2.3. Characterisation of nanocomposites

2.3.1. X-ray diffraction (XRD)

XRD experiments were conducted on a Philips X'pert Pro X-ray diffraction instrument that employed K-α radiation (λ = 1.5405 Å) and performed from 0.1 to 30.00°. The scanning rate was 0.017°/min.

2.3.2. Fourier transform infrared (FT-IR) spectroscopy

FT-IR Spectra of samples were collected on a Perkin–Elmer 1600 FT-IR spectrometer from 400 to 4000 cm^{-1} with a nominal resolution of 2 cm^{-1}. For each spectrum 64 runs were collected and averaged. The clay specimen were prepared by adding approximately 1% of the sample powder to dry KBr powder and pressed into disc of 13 mm in diameter and 1–2 mm thickness. Polymer/clay nanocomposite samples were tested by directly casting a thin film from a dilute solution on NaCl pellet.

2.3.3. Differential scanning calorimetry (DSC)

Thermal behaviour of PEO and PEO/clay nanocomposites was studied with DSC (TA instruments Q100 series).

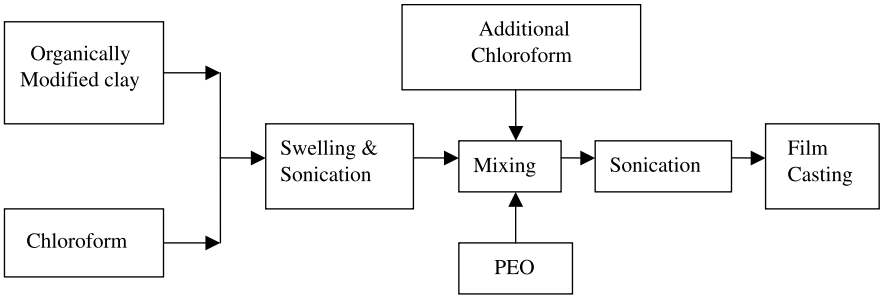

Fig. 2. Schematic Overview of the PEO/clay nanocomposite preparation.

About 15 mg of sample was placed in an aluminium pan and heated from room temperature to 100 °C at 5 °C/min. The reference was an empty aluminium pan.

Melting point (T_m), crystallization temperature (T_c) and enthalpy of crystallization (ΔH_c) was calculated as the maximum position of the endothermic peak and the area of crystallization curve under DSC thermogram.

2.3.4. Dynamic mechanical analysis (DMA)

DMA for the nanocomposites was carried out using a DMTA MK IV, Rheometric scientific instrument at a fixed frequency of 1 Hz from −90 to 40 °C with a heating rate of 5 °C/min in tensile mode. The sample size was 30 mm × 5 mm × 0.5 mm.

2.3.5. Tensile testing

Rectangular nanocomposites thin films were die cut with a rectangular die and tested in a Hounsfield universal testing machine (UTM) (Model 1150). The gauge length was kept 50 mm. The width and thickness of the samples were kept 10 and 0.2 mm, respectively. The cross head speed was 50 mm/min. The quoted results are the average from five samples of one particular clay loading in each case.

2.3.6. Polarized optical microscopy

The hot stage optical microscopy was performed on a Reico optical microscope in which two polarizers are aligned. The sample was heated from room temperature to 100 °C at 5 °C/min and then cooled back slowly at a rate of 2 °C/min to room temperature and the images were taken at a magnification of ×500.

3. Results and discussion

The most important question in this study is whether the nanocomposites are formed or not. An important characterization of nanocomposites is X-ray diffraction. The X-ray technique is often applied to identify intercalated structures through Bragg's relation

$$\lambda = 2d \sin \theta$$

where λ corresponds to the wavelength of the X-ray radiation used ($\lambda = 1.5405$ Å), d corresponds to the spacing between specific diffraction lattice planes and θ is the measured diffraction angle. The d value corresponding to the (001) plane was utilized in this study.

Fig. 3(a) represents the X-ray diffraction patterns for organically modified clay and the nanocomposite containing 7.5% clay without sonification. The clay shows the d_{100} peak at

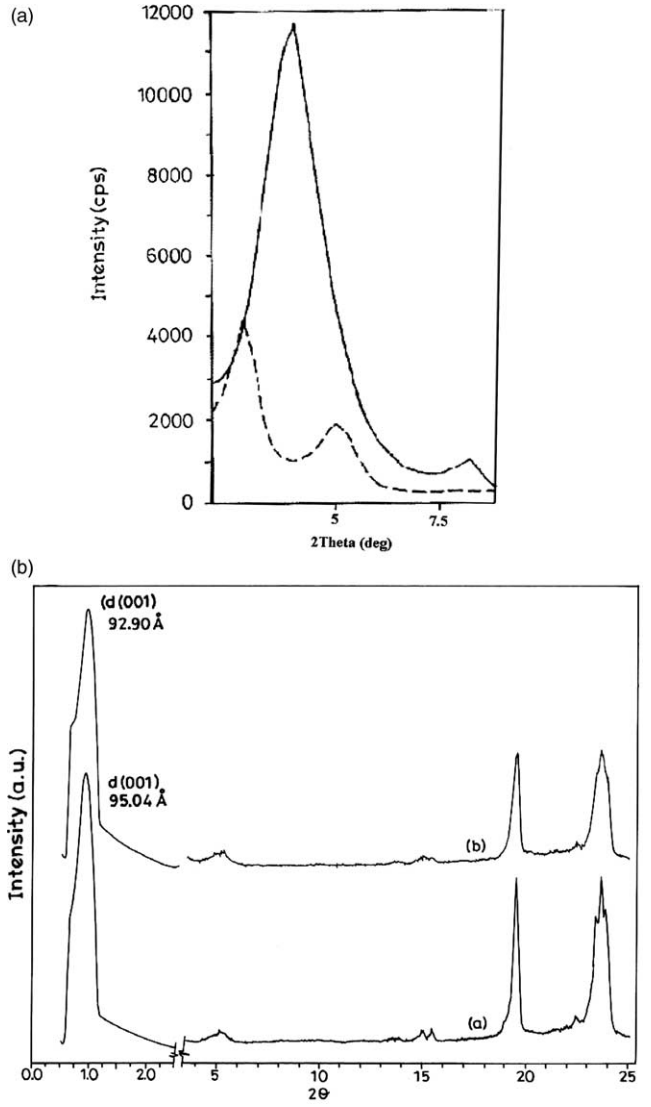

Fig. 3. (a) XRD plot of organoclay and 7.5% clay containing nanocomposites (b) XRD plots of a) 5% and b) 10% clay containing nanocomposite made using sonication.

$2\theta = 3.9$ which corresponds to a d-spacing of 2.20 nm. This indicates that modification of clay with organic ions not only makes the clay surface hydrophobic but results in a tremendous increase in d-spacing (d-space for untreated clay < 1 nm), which facilitates the penetration of PEO into the interlayer galleries [4,5]. In case of the composite sample, the basal spacing of clay is increased from 2.20 to 3.21 nm as the diffraction angle shifts from $2\theta = 4.0$ to 2.7 for the d_{001} peak. This indicates the formation of intercalated nanocomposite [4,5].

The nanocomposite samples were made by the method using sonication as described earlier. XRD studies of nanocomposite samples containing 5 and 10% by weight of clay indicates (Fig. 3(b)) that the d-spacing increases up to 9.5 nm as a result of sonication. Application of ultrasonication helps the clay to swell so that it is readily intercalated in the clay galleries and provides more energy and causes further separation and dispersion [31]. Hence, all further testing were carried out for samples after sonication.

The polymer/clay nanocomposite samples were also characterized by FT-IR spectroscopy. FT-IR spectroscopy provides important information regarding the difference between polymer and polymer clay hybrid. The FT-IR spectra of PEO/organo clay have been recently studied [11,17,23,29,31]. Results in our study do not, however, show the same results as in previous reports. The FT-IR spectra of pure PEO, organic clay, and a nanocomposite sample are shown in Fig. 4 and all the important absorption bands and their assignments are listed in Table 1.

Pure PEO shows a large broad band of asymmetric $-CH_2$ stretching between 3000 and 2750 cm^{-1} with the two narrow bands at 2739 and 2693 cm^{-1}. In the nanocomposite the band broadens between 3000 and 2800 cm^{-1}, whereas the narrow peaks disappear. In this region, the characteristic peaks of PEO which appear at 2793 and 2952 cm^{-1} are shifted to 2800 and 2936 cm^{-1}. The peaks in PEO at 1342 cm^{-1} shifted to 1347 cm^{-1} in intercalated hybrids. In a previous study by Shen et al. [23] similar observations are highlighted. This

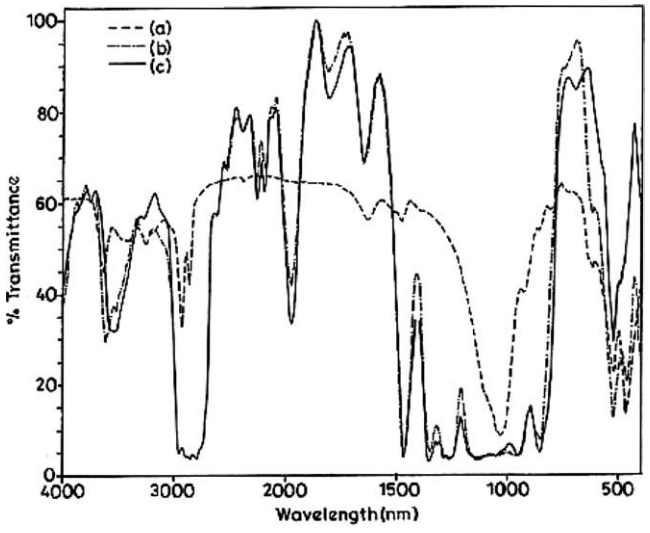

Fig. 4. FTIR spectra of (a) Organo clay (b) PEO/Clay nanocomposite containing 15 wt % clay and (c) Pure PEO.

Table 1
IR absorption bands and their assignment of PEO and PEO/clay nanocomposite (4000–400 cm^{-1})

Frequency (cm^{-1})	Assignment	Material
3000–2750	$\nu(CH_2)_a$	PEO
2952	$\nu(CH_2)_a$	PEO
2936	$\nu(CH_2)_a$	Nanocomposite
2800	$\nu(CH_2)_a$	Nanocomposite
2793	$\nu(CH_2)_a$	PEO
2739	$\nu(CH_2)_a$	PEO
2693	$\nu(CH_2)_a$	PEO
1358	$\Delta(CH_2)_a$	PEO
1342		PEO
1347		Nanocomposite
1320	$\nu(CH_2CH_2)$	PEO
1116	$\nu(C–O–C)_a$	PEO, nanocomposite
962 → 953	$r(CH_2)_a$	PEO, nanocomposite
842 → 849	$r(CH_2)_a$	PEO, nanocomposite

Mode assignment: ν (stretching), Δ (bending), r (rocking). The subscripts a and s denote asymmetric and symmetric motion wrt the two-fold axis perpendicular to the axis of the helix passing through O atom or through the centre of the C–C bond.

observation can be attributed to the ion dipole interaction of the interlayer cation of clay and the oxygen atoms of oxyethylene units [23,29]. The peaks near 862 and 842 cm^{-1} are assigned to the CH_2 rocking vibrations of methylene groups in the gauche conformation required for the helical conformation [17,29], so it is generally believed that virgin PEO is in a helical conformation. The absence of the characteristic PEO peak at 1320 cm^{-1} assigned to CH_2 vibrations of the ethylene group in the trans conformation as referred to by Ruiz-Hitzky et al. and Papke et al. [32] also confirms the helical structure of PEO. In Fig. 10 it is seen that the PEO peak at 842 cm^{-1} is shifted to 849 cm^{-1} in the intercalated hybrid which is assigned to the CH_2 asymmetric rocking vibration. The peaks at 1279 and 1241 cm^{-1} in PEO merge to give a single peak near 1276 cm^{-1} in the case of the nanocomposite.

In the region of 1300–900 cm^{-1}, we note peaks getting broader with the addition of organic clay, particularly the 1116 cm^{-1} peak in PEO which is for asymmetric stretching of the C–O–C groups [31] broadens while the 962 cm^{-1} peak shifts to a lower frequency of 953 cm^{-1}. It is also found that peaks apparent at 945 and 842 cm^{-1} which have been related to helical structure of PEO [23] are present in PEO only and not in the nanocomposite sample. This indicates that in the nanocomposite the helical structure of PEO in distorted/perturbed as a result of intercalation.

DSC analysis is generally one of the most convenient methods for analyzing first order transition like melting and crystallization. The nanocomposite samples with varying concentration of clay were subjected to DSC analysis and the thermograms are shown in Fig. 5. Presence of an intense melting peak indicates the semicrystalline nature of the polymer. From the DSC plots the melting point and heat enthalpy of crystallization were determined and are presented in Fig. 6. It was found that the melting point and heat of crystallisation (% crystallinity X_c) initially increases at lower concentration upto 2.5% of loading and decreases with further

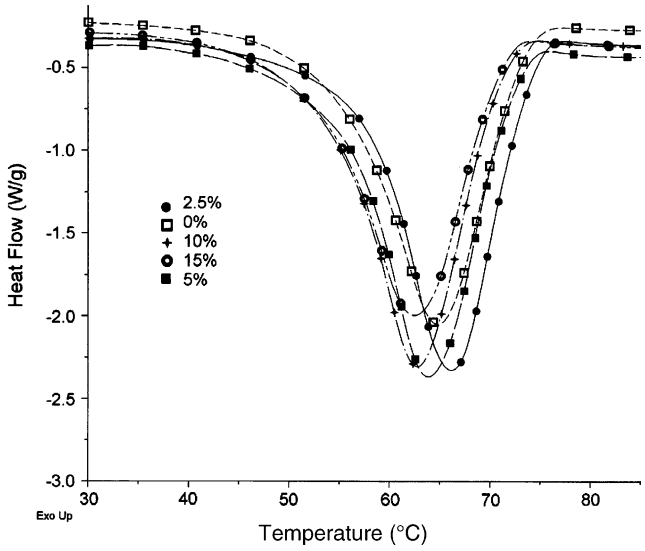

Fig. 5. DSC scan of PEO/clay nanocomposites with varying concentration of clay.

increase in clay concentration. The initial increase in T_m and X_c is attributed to the fact that clay platelets act as nucleating centres and favour crystallization by providing a higher level of nucleation density. Reduction in X_c is of particular interest as these composites can be used as solid polymer electrolytes by adding a suitable alkali metal ions, where it has been established that only the amorphous phase of PEO contribute to ionic conductivity [18]. The decrease in X_c with addition of clay can be explained by considering two possibilities like slowing down of kinetics of crystallisation and blockage of crystalline growth front caused by the clay platelets, dispersed in an irregular array in the nanocomposite as evident from hot stage microscopy studies as well. The polarized optical microphotographs for pure PEO and composite containing 5% clay are shown in Fig. 7(a) and (b). In Fig. 7(a), it can be seen that the virgin PEO, upon crystallization, forms distinct crystalline spherulites of considerable size. The presence of clay hinders the cystallisation as evident from the Fig. 7(b)

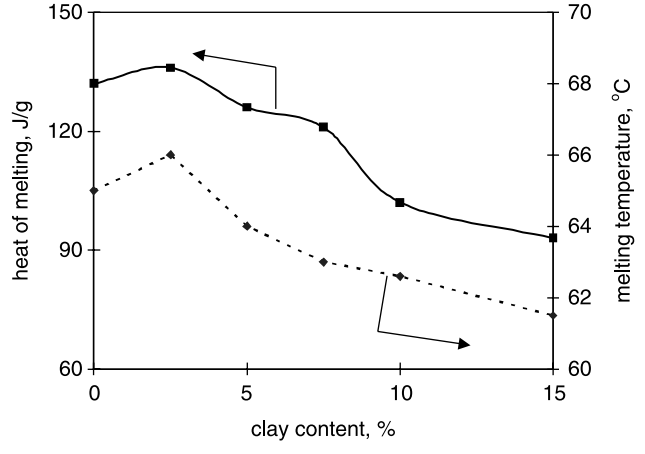

Fig. 6. Heat of melting and melting point of PEO/clay nanocomposites as a function of clay content.

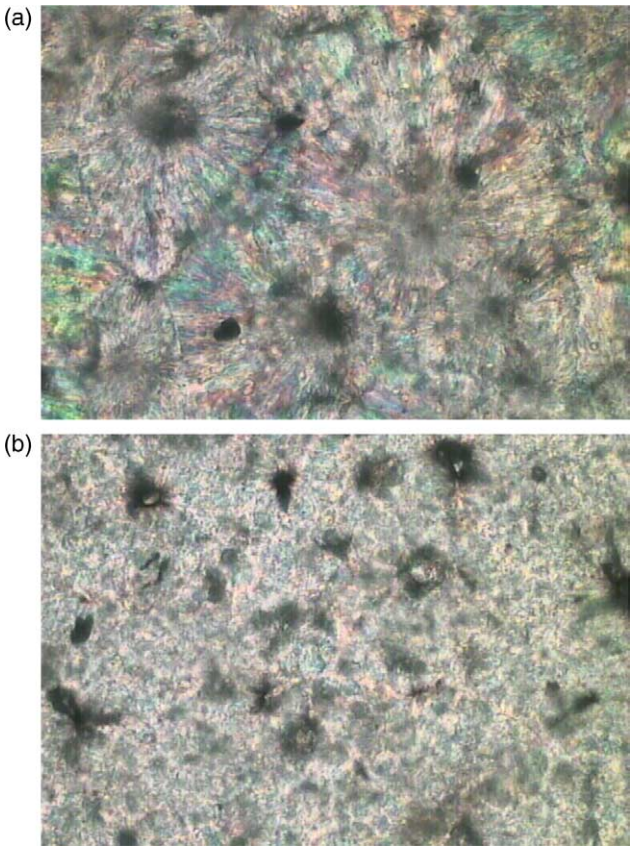

Fig. 7. Polarized optical micrograph (x 500) of pure PEO and 5% clay containing nanocomposite.

where the nanocomposite having 5 wt% clay shows spherulites of smaller size. Both the samples were crystallized in the same condition; cooling of the PEO melt at 100 °C at a rate of 2 °C/min. Since sufficient time has been given for crystallization, we believe that the decrease in crystallinity is due to the fact that at higher concentration of clay, the clay platelets stops the growing crystalline lamellae to grow in size in a particular direction.

The crystallization behaviour has been investigated for PEO/clay nanocomposites. The results are contradicting, Chen et al. [18] reported that crystallinity initially increases with incorporation of clay as the clay platelets act as nucleation centres and decreases with further addition of clay due to hindrance offered by randomly oriented clay. Loyens et al. [22], however, reported reduction of crystallinity even at clay concentration less than 1 wt%. In our study we have observed an initial increase in crystallinity followed by the reduction thereby supporting the work by Chen et al. [18].

In order to study the effect of incorporation of clay on the viscoelastic properties of PEO/clay nanocomposite, pure PEO and nanocomposite samples were subjected to DMA. The loss tangent vs. temperature and dynamic modulus vs. temperature plots for pure PEO and 7.5% clay containing nanocomposite are shown in Fig. 8. As the temperature is increased, it is observed that the damping goes through a maximum in T_g. The damping is low below T_g as the chain segment in that region is frozen. In the glass transition region, on the other hand, the

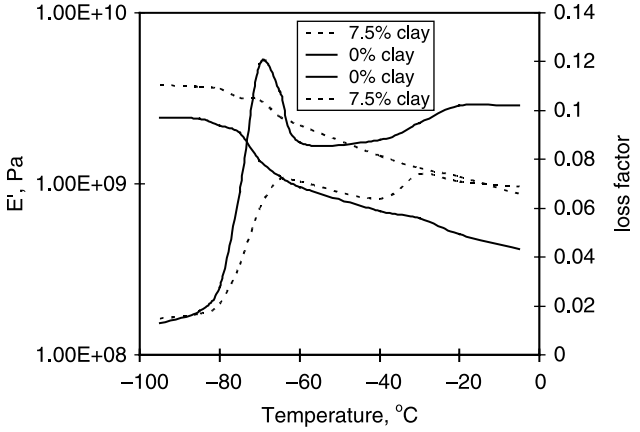

Fig. 8. Dynamic mechanical analysis of pure PEO and PEO/clay nanocomposite.

damping is high because of the initiation of micro-Brownian motion of the molecular chain segments. However, all the segments will not be able to take part in such relaxation together. A frozen-in segment can store much more energy for a given deformation than a free to move rubbery segment. Thus, every time a stressed frozen-in segment becomes free to move, its excess energy is dissipated. Micro-Brownian motion is concerned with the cooperative diffusional motion of the main chain segments. The maximum damping occurs at T_g where most of the chain segments take part in this co-operative motion under harmonic stress. The loss factor decreases above T_g because the molecular segments are free to move and consequently there is little resistance to flow.

A slight shift in loss tangent peak towards higher temperature was observed in case of the nanocomposite compared to pure PEO. This can be attributed to the confinement of polymer chains as a result of intercalation into the interlayer gallery of the clay. The increase in stiffness is also reflected in reduction in the loss peak height. A similar observation was reported for epoxy/clay nanocomposite using the same clay [3]. The loss peak was found to become broad due to incorporation of clay. This suggests that the clay introduces some kind of relaxation modes of PEO chain [33]. The storage modulus at all the temperature was found to be higher for nanocomposite compared to the pure PEO. Also, the change in storage modulus at T_g becomes smaller with the incorporation of clay. These are again the outcome of intercalation of the PEO chain.

The tensile test was conducted in order to obtain an idea of the effect of intercalation on the mechanical behaviour of nanocomposites with different clay loading. The stress–strain diagram of PEO and some nanocomposite samples are shown in Fig. 9. The stress–strain plots are like of typical plastics showing yield point and necking. The tensile strength and tensile modulus determined from stress–strain plots as a function of clay content are presented in Fig. 10. One can see from Fig. 9 that tensile strength increases with the incorporation of clay, attains a maximum value of 13.7 MPa at 12.5 wt% of clay, followed by a sharp decrease up to 20 wt% of clay. Above 20 wt% of clay the nanocomposite sample show

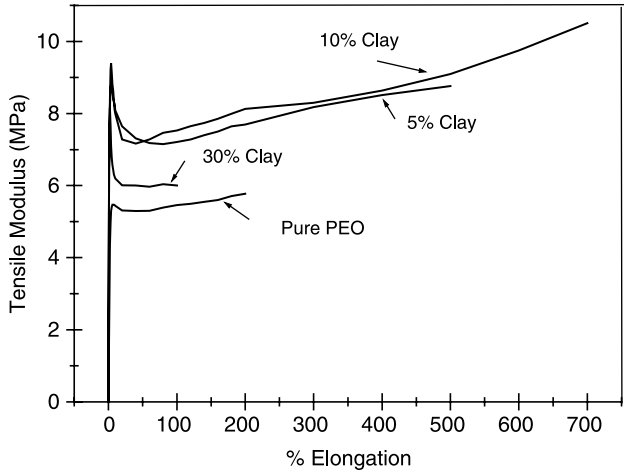

Fig. 9. Typical Stress-Strain diagram for PEO/clay nanocomposites.

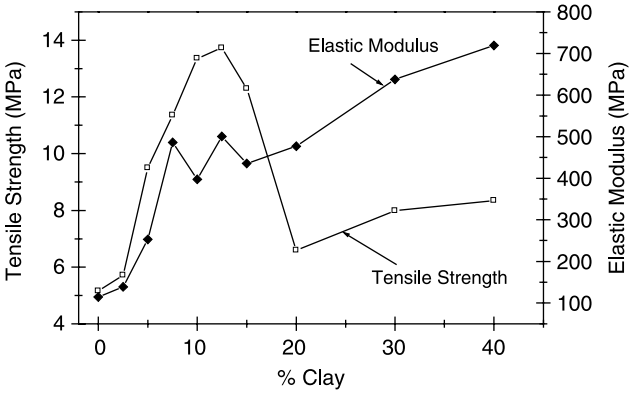

Fig. 10. Effect of clay loading on tensile strength and elastic modulus of PEO/clay nanocomposites.

almost the same strength as that of the unmodified PEO. This indicates that incorporation of clay up to an optimum level resulted in a considerable reinforcing effect. It is interesting to note that both tensile strength and % elongation increases simultaneously as evident from stress–strain curve (Fig. 9), i.e. improvement in mechanical property is achieved in both respects. However, at high loading of PEO the organo clay behaves as an ordinary filler with little improvement in strength, although modulus increases with increase in clay concentration due to the increase in rigidity. It can be said that at higher clay content the response to the extension under load is mainly governed by the hard and brittle clay and the intercalated PEO chains, which are not as extended as freely the PEO chains that are not intercalated. The deterioration of mechanical properties at higher clay concentration was also observed by Toyota researchers [1,2].

4. Conclusion

PEO/clay nanocomposites were synthesized using an a polar organo clay by a solution intercalation method. Intercalation is achieved by simple mechanical mixing and the extent of intercalation increases due to sonication. The basal spacing of

9.5 nm was achieved by the present method. Strong reinforcing effect was observed for clay content up to 12.5 wt% and after which the behaviour is like an ordinary filler. Hence, the concentration of clay plays an important role. Crystallinity in general tends to decrease with the addition of clay, which is beneficial for its application as electrolyte in association with alkali metal ions. Based on the results of FT-IR studies the presence of a distorted helical structure of PEO in the nanocomposite is confirmed.

References

[1] Usuki A, Kojima Y, Kawasumi M, Okoda A, Fukushima Y, Kurauchi T, et al. J Mater Res 1993;8:1185.
[2] Kawasumi M. J Polym Sci, Polym Chem 2004;42:819.
[3] Ratna D, Manoj NR, Singh Raman RK, Varley R, Simon GP. Polym Int 2003;52(9):1403.
[4] Frohlich J, Thomann R, Mulhaupt R. Macromolecule 2003;36:7205.
[5] Becker O, Varley RJ, Simon GP. Polymer 2002;43:4365.
[6] Karger-Kocsis J, Gryshchuk O, Frohlich J, Mulhaupt R. Compos Sci Technol 2003;63(14):2045.
[7] LeBaron PC, Wang Z, Pinnavaia TJ. Appl Clay Sci 1999;15:11.
[8] Giannelis EP. Adv Mater 1996;8:29.
[9] Carrado KA, Xu L. Chem Mater 1998;10:1440.
[10] Kawasumi M, Usuki A, Okada A, Karauchi T. Mol Cryst Liq Cryst 1996; 281:91.
[11] Ruiz-Hitzky E, Aranda P. Adv Mater 1990;2:545.
[12] Ruiz-Hitzky E, Aranda P, Casal B, Galvan JC. Adv Mater 1995;7:180.
[13] Lemmon JP, Lerner MM. Chem Mater 1994;6:207.
[14] Shen Z, Simon GP, Cheng YB. Polym Eng Sci 2002;42:2369.
[15] Beake BD, Chen S, Hall JB, Gao F. J Nanosci Nanotechnol 2002; 2(1):73.
[16] Choi HJ, Kim SG, Hyun YH, Jhon MS. Polym Prepr 2000;41:1183.
[17] Aranda P, Ruiz-Hitzky E. Chem Mater 1992;4:1395.
[18] Chen HW, Chang FC. Polymer 2001;42:9763.
[19] Riley M, Fedkiw PS, Khan SA. J Electrochem Soc 2002;149:A667.
[20] Vaia RA, Vasudevan S, Kraweic W, Scanlon LG, Giannelis EP. Adv Mater 1995;7:154.
[21] Wen Z, Gu Z, Itoh T, Lin Z, Yamamoto O. J Power Sources 2003;119: 427.
[22] Loyens W, Patric J, Maurer FHJ. Polymer 2005;46:903.
[23] Shen Z, Simon GP, Cheng YB. Polymer 2002;43:4251.
[24] Theng BKG. Formation and properties of clay–polymer complexes. New York: Elsevier; 1979.
[25] Chen B, Evans JRG. J Phys Chem B 2004;108:14986.
[26] Aranda P, Ruiz-Hitzky E. Acta Polym 1994;45:59.
[27] Kwiatkowski J, Whittaker AK. J Polym Sci, Part B: Polym Phys 2001;39: 1678.
[28] Hackett E, Manias E, Giannelis EP. Chem Mater 2000;12:2161.
[29] Aranda P, Mosqueda Y, Perez-Cappe E, Ruiz-Hitzky E. J Polym Sci, Part B: Polym Phys 2003;41:3249.
[30] Chen HW, Chiu CY, Chang FC. J Polym Sci, Part B: Polym Phys 2002; 40:1342.
[31] Chen C, Tolle TB. J Polym Sci, Polym Phys 2004;42:3891.
[32] Papke BL, Ratner MA, Shriver DF. J Phys Chem Solids 1981;42:493.
[33] Ogata N, Kawakage S, Ogihara T. Polymer 1997;38:5115.